

 Open access • Posted Content • DOI:10.20944/PREPRINTS201911.0240.V1

## Improving center vortex detection by usage of center regions as guidance for the direct maximal center gauge — [Source link](#)

Rudolf Golubich, Manfried Faber

**Published on:** 05 Dec 2019 - [arXiv: High Energy Physics - Lattice](#)

**Topics:** [Vortex](#), [Chiral symmetry breaking](#) and [Gauge \(firearms\)](#)

Related papers:

- [Improving center vortex detection by usage of center regions as guidance for the direct maximal center gauge](#)
- [The Road to Solving the Gribov Problem of the Center Vortex Model in Quantum Chromodynamics](#)
- [The road to solving the Gribov problem of the center vortex model in quantum chromo dynamics](#)
- [Center vortices and the Gribov horizon](#)
- [The vortex-finding property of maximal center \(and other\) gauges](#)

Share this paper:    

View more about this paper here: <https://typeset.io/papers/improving-center-vortex-detection-by-usage-of-center-regions-2iqs1v9iwz>

Article

# Improving Center Vortex Detection by Usage of Center Regions as Guidance for the Direct Maximal Center Gauge

Rudolf Golubich  and Manfred Faber \* 

Atominstytut, Technische Universität Wien, Operngasse 9, A-1040 Wien, Austria; rudolf.golubich@gmail.com

\* Correspondence: faber@kph.tuwien.ac.at

Received: 19 November 2019; Accepted: 9 December 2019; Published: 11 December 2019



**Abstract:** The *center vortex model* of quantum chromodynamic states that vortices, a closed color-magnetic flux, percolate the vacuum. Vortices are seen as the relevant excitations of the vacuum, causing confinement and dynamical chiral symmetry breaking. In an appropriate gauge, as *direct maximal center gauge*, vortices are detected by projecting onto the center degrees of freedom. Such gauges suffer from Gribov copy problems: different local maxima of the corresponding gauge functional can result in different predictions of the string tension. By using nontrivial center regions—that is, regions whose boundary evaluates to a nontrivial center element—a resolution of this issue seems possible. We use such nontrivial center regions to guide simulated annealing procedures, preventing an underestimation of the string tension in order to resolve the Gribov copy problem.

**Keywords:** quantum chromodynamics; confinement; center vortex model; string tension; Gribov copy problem

**PACS:** 11.15.Ha; 12.38.Gc

## 1. Introduction

First proposed by Hooft [1] and Cornwall [2] the *center vortex model* gives an explanation of confinement in non-Abelian gauge theories. It states that the vacuum is a condensate of quantized magnetic flux tubes, the so-called *vortices*. The vortex model is able to explain the following:

- Behavior of Wilson loops, see [3];
- Finite temperature phase transition  $\rightarrow$  Polyakov loops
- Orders of phase transitions in SU(2) and SU(3);
- Casimir scaling of heavy-quark potential, see [4];
- Spontaneous breaking of scale invariance, see [5];
- Chiral symmetry breaking, see [6,7]  $\rightarrow$  quark condensate;

but suffers from Gribov copy problems: predictions concerning the string tension depend on the specific implementation of the gauge fixing procedure, see [8,9].

In this work, an explanation of the problem is given before an improvement of the vortex detection is presented.

Center vortices are located by P-vortices, which are identified in direct maximal center gauge, the gauge which maximizes the functional

$$R^2 = \sum_x \sum_\mu | \text{Tr}[U_\mu(x)] |^2 . \quad (1)$$

The projection onto the center degrees of freedom

$$Z_\mu(x) = \text{sign Tr}[U_\mu(x)] \tag{2}$$

leads to plaquettes with nontrivial center values, P-plaquettes which form P-vortices, and closed surfaces in dual space. This procedure can be seen as a best fit procedure of a thin vortex configuration to a given field configuration [3,10], see Figure 1.

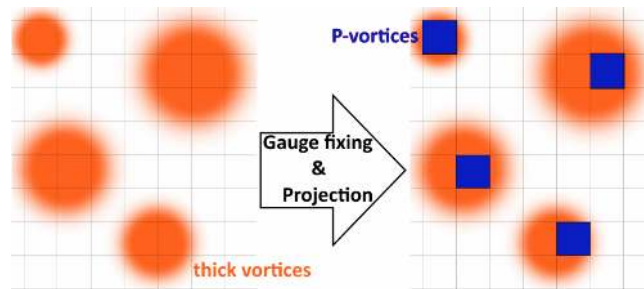


**Figure 1.** Vortex detection as a best fit procedure of P-Vortices to thick vortices shown in a two-dimensional slice through a four dimensional lattice.

The way P-vortices locate thick vortices is called *vortex finding property*.

Center vortices can be directly related to the string tension: the flux building up the vortex contributes a nontrivial center element to surrounding Wilson loops, see Figure 2.

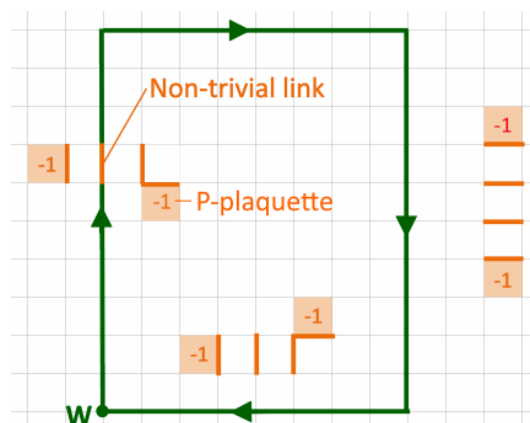


**Figure 2.** Each P-plaquette contributes a nontrivial center element to surrounding Wilson loops.

The behavior of Wilson loops can be explained and a nonvanishing string tension extracted by using the density  $\rho_u$  of uncorrelated P-plaquettes per unit volume

$$\langle \frac{1}{2} \text{Tr}(\mathbf{W}(R, T)) \rangle = [-1 \rho_u + 1 (1 - \rho_u)]^{R \times T} = e^{\ln(1-2\rho_u) R \times T} \Rightarrow \sigma = -\ln(1 - 2 \rho_u). \tag{3}$$

The string tension can also be calculated by Creutz ratios

$$\chi(R, T) = -\ln \frac{\langle \mathbf{W}(R + 1, T + 1) \rangle \langle \mathbf{W}(R, T) \rangle}{\langle \mathbf{W}(R, T + 1) \rangle \langle \mathbf{W}(R + 1, T) \rangle}. \tag{4}$$

From  $\langle \mathbf{W}(R, T) \rangle \approx e^{-\sigma R T - 2 \mu (R+T) + C}$ , it follows for sufficiently large R and T that  $\chi(R, T) \approx \sigma$ . Creutz ratios for center-projected Wilson loops are expected to give correct values for  $\sigma$  if the vortex finding property is given.

The problem with the direct maximal center gauge is that different local maxima of the gauge functional R can lead to different predictions concerning the string tension in center-projected

configurations [8,9]. An improvement in the value of the gauge functional results in an underestimation of the string tension, as can be seen in Figure 3.

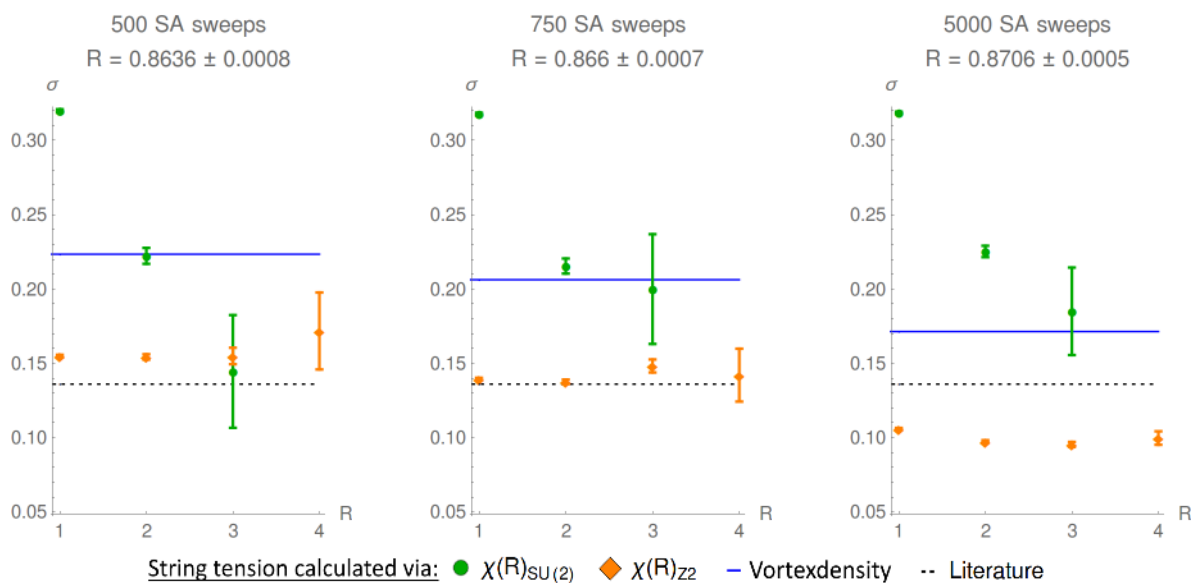


**Figure 3.** The string tension, calculated via Creutz ratios of the full theory  $\chi(R)_{SU(2)}$ , the center-projected theory  $\chi(R)_{Z2}$ , and the vortex density. By increasing the number of simulated annealing sweeps, a better value of gauge functional is reached, but the string tension is underestimated by  $\chi(R)_{Z2}$ . The data was calculated in lattices of size  $12^4$  (left),  $12^4$  (middle), and  $14^4$  (right) in Wilson action. The vortex density was not corrected for correlated P-plaquettes, hence, it is overestimated.

In fact, preliminary analyses show that the string tension decreases linearly with an improvement in the value of the gauge functional.

We believe that this is caused by a failing gauge-fixing procedure during which the vortex finding property is lost. If the P-vortices fail to locate thick vortices, the string tension will be underestimated by  $\chi(R)_{Z2}$ , see Figure 4.

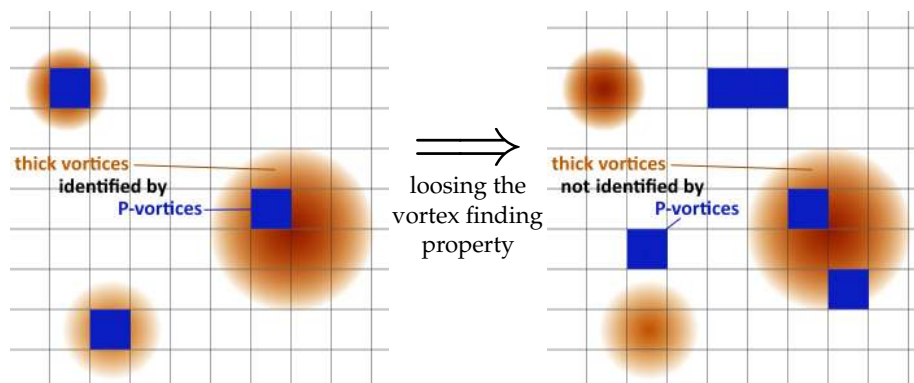


**Figure 4.** When P-vortices no longer locate thick vortices, we speak of a loss of the *vortex finding property*. The figure shows a two-dimensional slice through a four-dimensional lattice.

A failing vortex detection can result in vortex clusters disintegrating into small vortices consisting only of correlated P-plaquettes. This causes a misleadingly high vortex density.

The loss of the vortex finding property can be avoided by using the information about center regions, that is, regions enclosed by a Wilson loop that evaluate to center elements.

Center regions can be related to a non-Abelian generalization of the Abelian Stokes theorem:

$$\begin{aligned}
 P \exp \left( i \oint_{\partial S} A_\mu(x) dx^\mu \right) &= \mathcal{P} \exp \left( \frac{i}{2} \int_S \mathcal{F}_{\mu\nu}(x) dx^\mu dx^\nu \right), \\
 \mathcal{F}_{\mu\nu}(x) &= U^{-1}(x, O) F_{\mu\nu}(x) U(x, O), \quad U(x, O) = P \exp \left( i \int_l A_\eta(y) dy^\eta \right),
 \end{aligned}
 \tag{5}$$

with  $P$  denoting path ordering,  $\mathcal{P}$  "surface ordering", and  $l$  being a path from the base  $O$  of  $\partial S$  to  $x$ , see [11]. The left hand side of (5) can be identified as the evaluation of a Wilson loop spanning the surface  $S$ . The right-hand side can be expressed using plaquettes:  $U_{\mu\nu}(x) = \exp (ia^2 F_{\mu\nu} + \mathcal{O}(a^3))$ , with lattice spacing  $a$ , see [12]. With these ingredients, the non-Abelian Stokes theorem reads in the lattice, as shown in Figure 5:



Figure 5. Factoring a Wilson into factors of plaquettes using the non-Abelian Stokes theorem.

By finding center regions, that is, plaquettes within  $S$  that combine to bigger regions which evaluate to center elements, the Wilson loop spanning  $S$  can be factorized into a commuting factor, a center element, and an non-Abelian part, see Figure 6.

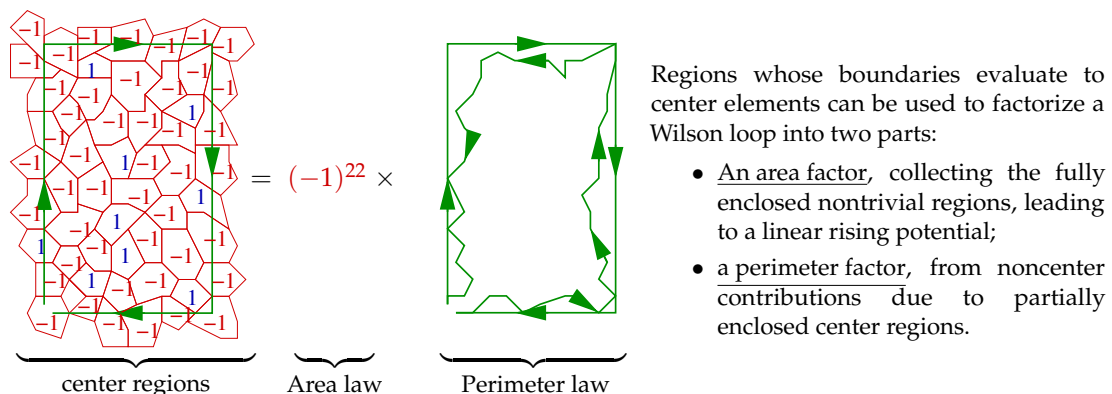


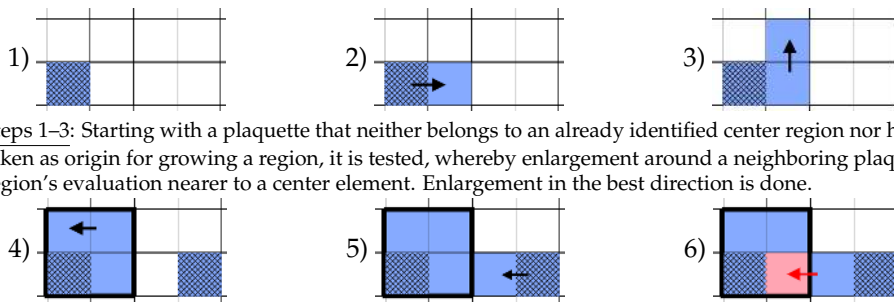
Figure 6. Center regions explain the coulombic behavior and the linear rise of the quark–antiquark potential as they lead to an area law and a perimeter law for Wilson loops.

The center regions capture the center degrees of freedom and can be directly related to the behavior of Wilson loops. It seems reasonable to demand that their evaluation should not be changed by center gauge or projection on the center degrees of freedom. We show that by preserving nontrivial center regions, the loss of the vortex finding property is prevented and the full string tension can be recovered.

## 2. Materials and Methods

The predictions of the center vortex model concerning the string tension in SU(2) gluonic quantum chromodynamic are analyzed by calculating the Creutz ratios after center projection in maximal center gauge. The gauge fixing procedure is based upon simulated annealing, maximizing the functional (1), that is, bringing each link as close to a center element as possible. The simulated annealing algorithms are modified so that the evaluation of center regions is preserved during the procedure: transformations resulting in nontrivial center regions projecting onto the nontrivial center element are enforced, and transformations resulting in nontrivial center regions projecting onto the trivial center element are prevented.

The detection of the nontrivial center regions of one lattice configuration is done by enlarging regions until their evaluation becomes the nearest possible to a nontrivial center element, see Figure 7.



Steps 1–3: Starting with a plaquette that neither belongs to an already identified center region nor has already been taken as origin for growing a region, it is tested, whereby enlargement around a neighboring plaquette brings the region’s evaluation nearer to a center element. Enlargement in the best direction is done.

Steps 4–6: If no enlargement leads to further improvement, a new enlargement procedure is started with another plaquette. With this enlargement, it is possible that it would grow into an existing region. The collision-handling described in the following is used to prevent this:



Step 7a: The evaluation of the growing region is nearer to a nontrivial centre element than the evaluation of the old region: delete the old region, only keeping the mark on its starting plaquette, and allow growing.

Step 7b: The growing region evaluates further away from a nontrivial centre element than the existing one: prevent growing in this direction and, if possible, enlarge in second best direction instead. Multiple collisions after growing are possible.

**Figure 7.** The algorithm for detecting center regions repeats these procedures until every plaquette either belongs to an identified region or has been taken once as starting plaquette for growing a region. The arrow marks the direction of enlargement. Plaquettes belonging to a region are colored, plaquettes already used as origin are shaded.

The algorithm starts with sorting the plaquettes of a given configuration by a rising trace of their evaluation. This stack is worked down plaquette by plaquette, enlarging each as far as possible by adding neighboring plaquettes. During this procedure, collisions of growing regions are prevented.

The regions identified this way comprise of many, whose evaluation deviates far from the center of the group. A set of nontrivial center regions has to be selected from the set of identified regions, only regions with traces smaller than  $Tr_{max}$  are taken into account. This parameter  $Tr_{max}$  has to be adjusted under consideration of the behavior of Creutz ratios, as shown in Figure 8, which are calculated after gauge-fixing and center projection.

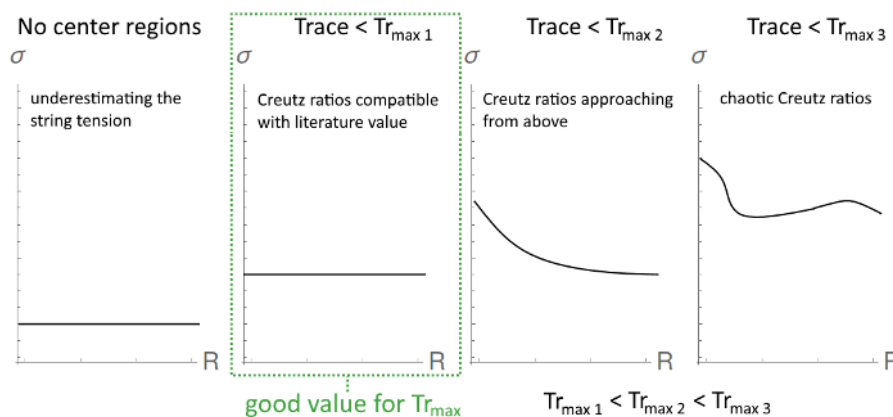


**Figure 8.**  $Tr_{max}$  can be fine-tuned by looking at the dependency of the Creutz ratios on the loop size  $R$ .

At low values of  $Tr_{max}$ , the Creutz ratios are expected to be nearly constant with respect to the loop size. With raising  $Tr_{max}$  they start to approach their asymptotic value from above and become chaotic with  $Tr_{max}$  chosen inappropriately high.

As the center degrees of freedom are expected to capture the long-range behavior, the Creutz ratios calculated in center-projected configurations are near to the correct value of the string tension already for small loop sizes. Hence, we chose  $Tr_{\max}$  as high as possible without causing the behavior of the Creutz ratios to approach the string tension from above.

The regions determined by this procedure are then used to guide the gauge-fixing procedure. The influence on the predicted string tension is analyzed by calculating the Creutz ratios in center-projected configurations.

### 3. Results

Here, we present the calculations of the center vortex string tension for different values of  $Tr_{\max}$  at  $\beta = 2.3$ . Similar results were obtained for  $\beta = 2.4$  and  $\beta = 2.5$ . In the following, only the Creutz ratios of the center-projected configurations  $\chi(R)_{Z2}$  are of relevance. The Creutz ratios of the full SU(2) theory  $\chi(R)_{SU(2)}$  and the calculations of the string tension based on the vortex density are calculated for comparison. They are only shown for the sake of completeness. All data was calculated with SU(2) Wilson action.

The Creutz ratios tend towards the literature value of the string tension with increasing number of simulated annealing steps with a  $Tr_{\max} = -0.985$ , whereas they clearly underestimate the string tension when center regions are ignored, see Figure 9.

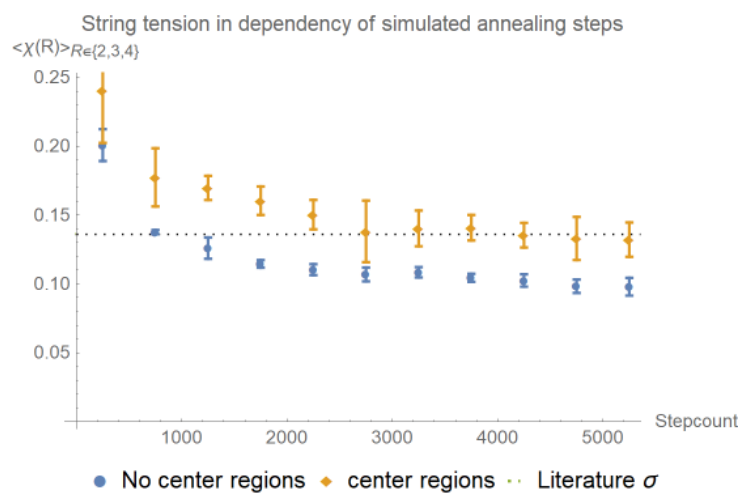


**Figure 9.** By preserving center regions, the Creutz ratios tend towards the literature value of string tension during the simulated annealing procedure. The data was calculated at  $\beta = 2.3$  in a  $12^4$  lattice with 100 configurations taken into account per datapoint. Displayed is the mean of  $\chi(2)$ ,  $\chi(3)$ , and  $\chi(4)$ . The increased error bars when center regions are preserved might be because the algorithm does not reach the exact local maxima, but fluctuates around it.

The full string tension can be easily recovered, although the value of the gauge functional is reduced, see Figure 10.

The upper three graphs show the calculations done for optimizing the value of  $Tr_{\max}$ . The final results, shown in the left graph in the lower row, are calculated with a value of  $Tr_{\max} = -0.985$ , that is, a value between the respective values of the left and middle graph in the upper line. The final results are compared with raw simulated annealing, that is, without preserving center regions shown in the right graph of the lower row. The large errors using center regions might result from fluctuations of the gauge functional around the maxima, which can not be reached due to the constraint of the preservation of center regions: further approaches to the local maxima of the gauge functional are therefore prevented.

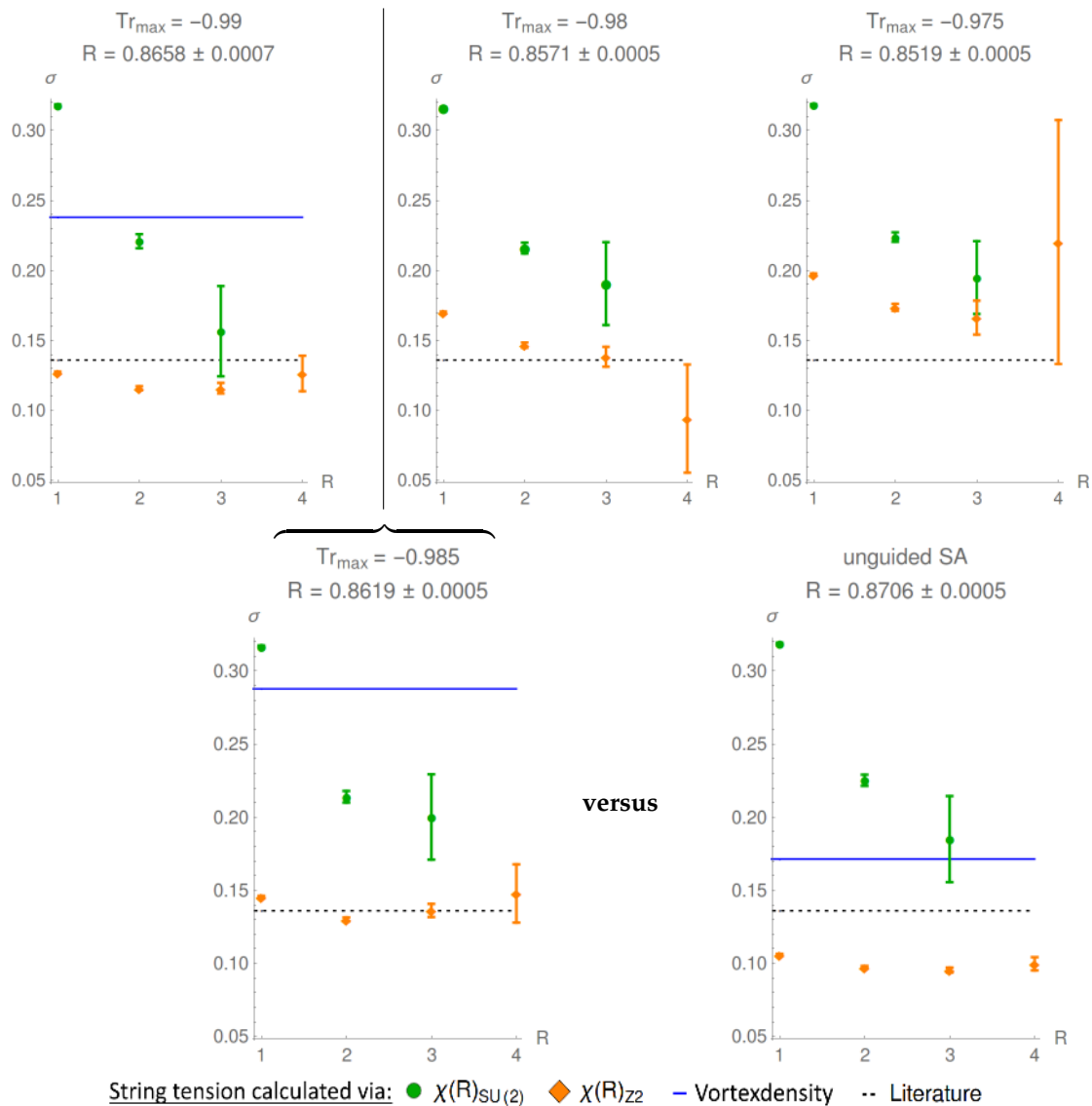


**Figure 10.** Optimization of  $Tr_{max}$  in the upper line and final results for the guided simulated annealing in the lower row at  $\beta = 2.3$ . The Creutz ratios were calculated with 300 Wilson configurations at  $\beta = 2.3$  in lattices of sizes  $12^4$  in the upper-left graph and  $14^4$  for the other graphs. The error bars are calculated with the one-deletion-Jackknife method. The optimal value of  $Tr_{max}$  was identified by taking into account the behavior of the Creutz ratios and found to be around  $Tr_{max} \approx -0.985$ , reducing the value of gauge functional from  $R = 0.871$  to  $0.862$ .

#### 4. Discussion

By preserving nontrivial center regions, the full string tension can be recovered and extracted from the center degrees of freedom in SU(2) quantum chromodynamics. The choice of the free parameter  $Tr_{max}$  based on the behavior of Creutz ratios does not give an unambiguous value, but merely an interval of good values of  $Tr_{max}$ . This arbitrariness has to be investigated in further work. Preliminary data already hints at a way to eliminate it. The concept of identifying gauge-independent observables evaluating to the relevant degrees of freedom and using them to guide the gauge-fixing procedure reduces the number of free parameters of the gauge transformation. It forces all differing local maxima of the gauge functional to incorporate specific, gauge-invariant properties that are related to the relevant degrees of freedom. This might be a solution to the Gribov copy problem wherever the gauge-fixing procedure is based upon a specific gauge functional. The algorithms presented can be easily extended into higher symmetry groups or modified to capture different degrees of freedom.



The procedures for identifying nontrivial center regions can also be used to reconstruct the thick vortices from P-plaquettes. This will allow further investigations of the color structure of vortices.

**Author Contributions:** Conceptualization, M.F.; Investigation, R.G.; Writing—original draft, R.G.; Writing—review editing, M.F.

**Funding:** This research received no external funding.

**Acknowledgments:** We thank Vitaly Bornyakov for the helpful discussions of the results.

**Conflicts of Interest:** The authors declare no conflict of interest.

## References

1. Hooft, G. On the phase transition towards permanent quark confinement. *Nucl. Phys. B* **1978**, *138*, 1–25. [[CrossRef](#)]
2. Cornwall, J.M. Quark confinement and vortices in massive gauge-invariant QCD. *Nucl. Phys. B* **1979**, *157*, 392–412. [[CrossRef](#)]
3. Del Debbio, L.; Faber, M.; Giedt, J.; Greensite, J.; Olejnik, S. Detection of center vortices in the lattice Yang-Mills vacuum. *Phys. Rev.* **1998**, *D58*, 094501. [[CrossRef](#)]
4. Faber, M.; Greensite, J.; Olejnik, S. Casimir scaling from center vortices: Towards an understanding of the adjoint string tension. *Phys. Rev.* **1998**, *D57*, 2603–2609. [[CrossRef](#)]
5. Langfeld, K.; Reinhardt, H.; Tennert, O. Confinement and scaling of the vortex vacuum of SU(2) lattice gauge theory. *Phys. Lett.* **1998**, *B419*, 317–321. [[CrossRef](#)]
6. Höllwieser, R.; Schweigler, T.; Faber, M.; Heller, U.M. Center Vortices and Chiral Symmetry Breaking in SU(2) Lattice Gauge Theory. *Phys. Rev.* **2013**, *D88*, 114505. [[CrossRef](#)]
7. Faber, M.; Höllwieser, R. Chiral symmetry breaking on the lattice. *Prog. Part. Nucl. Phys.* **2017**, *97*, 312–355. [[CrossRef](#)]
8. Bornyakov, V.G.; Komarov, D.A.; Polikarpov, M.I.; Veselov, A.I. P vortices, nexuses and effects of Gribov copies in the center gauges. Quantum chromodynamics and color confinement. In Proceedings of the International Symposium, Confinement 2000, Osaka, Japan, 7–10 March 2000, 2002; pp. 133–140.
9. Faber, M.; Greensite, J.; Olejnik, S. Remarks on the Gribov problem in direct maximal center gauge. *Phys. Rev.* **2001**, *D64*, 034511. [[CrossRef](#)]
10. Faber, M.; Greensite, J.; Olejnik, S. Direct Laplacian center gauge. *JHEP* **2001**, *11*, 053. [[CrossRef](#)]
11. Broda, B. Non-Abelian Stokes theorem. *arXiv* **1995**, arXiv:hep-th/9511150.
12. Gattringer, C.; Lang, C. *Quantum Chromodynamics on the Lattice: An Introductory*; Springer: New York, NY, USA, 2010.

**Sample Availability:** All data and Fortran source codes of the algorithms are available from the authors.



© 2019 by the authors. Licensee MDPI, Basel, Switzerland. This article is an open access article distributed under the terms and conditions of the Creative Commons Attribution (CC BY) license (<http://creativecommons.org/licenses/by/4.0/>).